International Journal of Information, Control and Computer Sciences
ISSN: 2517-9942
Vol:5, No:10, 2011

Measurement of Real Time Drive Cycle for Indian Roads and Estimation of Component Sizing for HEV using LABVIEW

Varsha Shah, Patel Pritesh, Patel Sagar, PrasantaKundu, RanjanMaheshwari

***Abstract*—**Performance of vehicle depends on driving patterns and vehicle drive train configuration. Driving patterns depends on traffic condition, road condition and driver behavior. HEV design is carried out under certain constrain like vehicle operating range, acceleration, decelerations, maximum speed and road grades which are directly related to the driving patterns. Therefore the detailed study on HEV performance over a different drive cycle is required for selection and sizing of HEV components. A simple hardware is design to measured velocity v/s time profile of the vehicle by operating vehicle on Indian roads under real traffic conditions. To size the HEV components, a detailed dynamic model of the vehicle is developed considering the effect of inertia of rotating components like wheels, drive chain, engine and electric motor. Using vehicle model and different Indian drive cycles data, total tractive power demanded by vehicle and power supplied by individual components has been calculated.Using above information selection and estimation of component sizing for HEV is carried out so that HEV performs efficiently under hostile driving condition. Complete analysis is carried out in LABVIEW.

***Keywords*—**BLDC motor, Driving cycle, LABVIEW Ultracapacitors, Vehicle Dynamics,

NOMENCLATURE

Notation	Description	Unit
A	Frontal Area Of A Vehicle.	m^2
A	Acceleration Of A Vehicle.	m/s^2
C_d	Air Drag Co-efficient.	-
C_{rf}	Rolling resistance co-efficient of the front wheel.	-
C_{rr}	Rolling resistance co-efficient of the rear wheel.	-
E_{EO}	Energy output from the storage unit during propulsion.	Joules
F_A	Aerodynamic drag force.	Newton
F_{ac}	Acceleration force.	Newton
f_b	Fraction of braking.	-
F_g	Grade force.	Newton
F_T	Total tractive force.	Newton
G	Acceleration due to gravity.	m/s^2
J_d	Moment of inertia of the driveline.	$Kg\text{-}m^2$
J_M	Moment of inertia of the motor.	$Kg\text{-}m^2$
J_w	Moment of inertia of the wheel/tire assembly.	$Kg\text{-}m^2$
J_e	Moment of inertia of internal combustion engine.	$Kg\text{-}m^2$
K	Regenerative brake fraction.	-
m_e	Effective mass of the vehicle.	Kg
m_v	Total mass of the test vehicle.	Kg
m_w	Mass of the wheel.	Kg
m_t	Mass of the tire.	Kg
N_F	Final drive gear ratio.	-
N_T	Transmission gear ratio.	-
P_{EO}	Power output from the energy storage unit during propulsion.	Watts
P_{EI}	Power input into energy storage during braking.	Watts
P_{BI}	Power input into brake system during braking.	Watts
P_{DO}	Power output from the driveline during propulsion.	Watts
P_{DI}	Power input into driveline during braking.	Watts
P_R	Power loss during regeneration.	Watts
P_{MO}	Power output from the motor during propulsion.	Watts
P_{MI}	Power Input into motor during braking.	Watts
P_{WO}	Power output from the wheel/tire assembly during propulsion.	Watts
P_{WI}	Power input into the wheel/tire assembly during braking.	Watts
P_{ICEO}	Power output from the ICE.	Watts
P_{ICEI}	Power input to the ICE.	
r_e	Outer radius of the wheel.	Meter
r_t	Outer radius of the tire.	Meter
r_w	Rolling radius of the wheel.	Meter
$w_{M/G}$	Speed Of the motor/generator output shaft.	Rpm
$T_{M/G}$	Torque of the motor/generator set.	N-m
T_{ICE}	Torque of the internal combustion engine.	N-m
Ρ	Density of the air.	(K_g/m^3)
Θ	Angle of the road from the horizontal axis.	rad
η_t	Transmission efficiency.	-
η_f	Final drive efficiency.	-
η_{ICE}	Efficiency of internal combustion engine.	-
$\eta_{M/G}$	Efficiency of motor/generator.	-
$\omega_{M/G}$	Angular speed of motor/generator.	rad
HEV	Hybrid electric vehicle.	-
FWD	Forward wheel drive vehicle.	-
RWD	Rear wheel drive vehicle.	-
AWD	All wheel drive vehicle.	-
ICE	Internal combustion engine.	-

Varsha Shah and Dr. PrasantaKundu is with Department of Electrical Engineering, S V National Institute of Technology, Surat, India. (e-mail: vas@eed.svnit.ac.in)Patel Pritesh M (e-mail:patel_pritesh05@yahoo.com)
Patel Sagar M (e-mail: sagar9150@gmail.com)PrasantaKundu (e-mail: pk@eed.svnit.ac.in) Patel Pritesh is a student of M.Tech in SVNIT, Surat and Patel Sager is a student of B.Tech in ADIT, Vallabh-vidhya Nagar.RanjanMaheshwari is with the department of Electrical Engineering, Government college of engineering, Kota, India. (E-mail: ranjan_alpi@hotmail.com).

I. INTRODUCTION

ROAD vehicles are immerging as the largest source of urban air pollution due to rapidly increasing numbers of vehicles & very limited use of emission control strategies. Sky rising cost of fuel as well as environment impact due to emission have drawn attention of many automobile manufacturing companies to divert their mind toward the development of a HEV. Maximum efforts in HEV research are on development of efficient and cost effective HEV propulsion system. Performance of the vehicle depends on the efficient drive train system as well as on the type of driving pattern i.e. type of roads and their physical condition, road traffic and driver behavior [1].

The driving cycle is a sequence of vehicle operating conditions i.e. ideal, acceleration, steady state (const. speed) and declaration with respect to time for a given city, region or a country. The driving pattern varies from city to city and from region to region [2]. Driving cycle can be categorized as synthesized and actual drive cycles [7]. The synthesized drive cycles like European, Japanese, California seven modes and Indian driving cycle are constructed from a number of constant acceleration and constant speed phase. As this cycles are complexes in nature, transition between various models are somewhat artificial in nature. This type of cycles are unsuitable for evaluating power required by vehicle due to its gentle acceleration, braking & long period spent in stationary mode. Actual driving cycles are derived from the operation of test vehicle on the road under real traffic condition. Actual drive cycle are best suitable for heterogeneous traffic condition which represent short acceleration & declaration which are the main mode of operation responsible for higher emission and fuel consumption.

Initially drive cycles was introduce in vehicle research to measure the fuel consumption and emission of the vehicle. Indian drive cycle (IDC) was formatted around late 1985 by the automotive research Association of India (ARAI) with speed and acceleration up to 42 km/h and 0.65m/s^2. IDC is a simulated drive cycle in a laboratory on test the vehicle. It assumes all vehicle activities to be homogeneous irrespective of variation in traffic and driving characteristic. Thus it does not represent the real world driving. Pune city drive cycle measurement was carried out for estimation of emission and fuel consumption of conventional vehicle

While designing and selecting a HEV configuration and component with minimum emission, the constrain impose on optimizing the component selection and sizing are vehicle range, acceleration, deceleration, maximum speed, road grades, level of emission, fuel economy, and amount of regenerative power during braking, and downhill operation. Almost all factors are directly related to the driving patterns of the vehicle.

Design Specification for HEV may be divided into two categories.

1) Hardware specification: User governed specification derived mostly from consumer demand. i.e. the acceleration, fuel economy and max speed. Using this sizing of electric motor, engine, transmission system, energy storage devices like batteries, ultracapacitor etc. can be done.

2) Software specification: Development of efficient power split algorithm between motor and ICE so that vehicle emission should be maintained within the regulation limit. This control algorithm also takes care of state of charge of battery & ultracapacitor as well as engine operation within the efficient modes.

There are two different types of approaches to define vehicle specifications, 1) Selective approach in which the optimal sizing of HEV or EV component will be done with selected driving Pattern. 2) General approach which customizes the hardware & software specification of HEV so that it perform reasonably well under diverge driving condition. This will not give any optimize result for any particular drive cycle.

[12] proposed evaluation of the merits of alternative vehicle design option using drive cycle. Feng & Marc worked on fuel economy of conventional Vehicle using drive cycle. Feng& of al. presented simulation result on the impacts of driving patterns on EV & HEV performance.

The focus of this paper is to understand and analyze the effect of real time Indian drive cycle on selction and sizing of HEV components. Three real time Indain drive cycles 1) Surat city drive cycle (Urban drive cycle), 2) State Highway drive cycle, 3) Expressed highway drive cycle are measured using microcontroller and LABVIEW. The dynamic model of HEV is developed in LABVIEW and using real time Indain drive cycle data maximum and average acceleration, maximum and average speed, total tractive power and torque and power generated under braking conditions are calculated in LABVIEW. Using a generalized approach estimation of component sizing for HEV is carried out for above mention three Indian drive cycles.

The objective of this paper is in three folds:

1) Modeling of vehicle dynamics considering effective mass of vehicle.

2) Measurement of real time Indian drive cycles by operating the test vehicle on different types of Indian roads.

3) Using drive cycle data and derived dynamic model of vehicle, power required by the vehicle under different operating conditions is calculated. Based on the above calculation estimation of component sizing is carried out for a vehicle which is to be hybridized.

II. Vehicle Dynamics

The test vehicle is configured as a parallel hybrid electric vehicle (FWD) as shown in Fig 2 and 4. The components of parallel HEV are ICE, transmission and gear system, electric motor(BLDC), DC-DC converter, inverter, batteries and ultracapacitor. The power requires to drive a vehicle depends on the following factors as shown in Fig (1) [11]:

1) Aerodynamic Drag: Equation (1) is the force due to the friction of the body moving through air.

$$F_A = \frac{1}{2}\,\rho\, C_d A V^2 \qquad (1)$$

2) Rolling Resistance: The rolling resistance is primarily due to the friction of the vehicle tyre on the road. The rolling resistance is approximately constant, and hardly depends on vehicle speed. The magnitude of rolling resistance depends mainly on the nature of road surface, types of tyre viz. pneumatic or solid rubber type and the weight of the vehicle and is given by (2).

$$F_r = [C_{rf} m_f + C_{rr}(1-m_r)]\, m_v\, g \cos\theta \qquad (2)$$

3) Grade Force: The force needed to drive the vehicle up a slope is given by (3).

$$F_g = m_v\, g \sin\theta \qquad (3)$$

4) Acceleration Force: According to Newton’s seconds law, acceleration force is given by (4)

$$F_{ac} = m_e\, a \qquad (4)$$

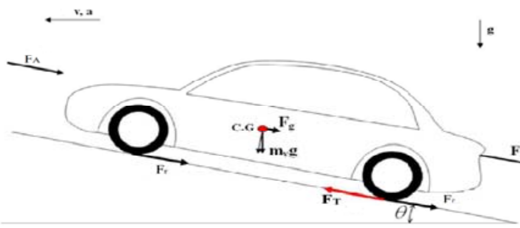

Fig 1 Forces acting on the vehicle

5) Effective Mass Of A Vehicle: All rotating components in a vehicle have rotating inertias, and have an effect on vehicle performance. Rotating inertia offered by the motor/generator, ICE, driveline and wheel/tire assembly are considered to calculate the effective mass of a vehicle which is given by (5).

$$m_e' = m_v + 4\frac{J_w}{r_w^2} + \frac{J_d N_T^2 N_F^2}{r_w^2}$$
$$m_e = m_e' + \frac{J_M N_T^2 N_F^2}{r_w^2} + \frac{J_c N_T^2 N_F^2}{r_w^2} \quad (5)$$

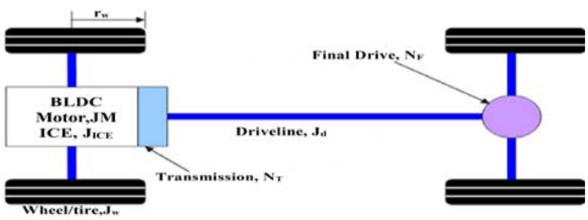

Fig 2 Schematic diagram of a vehicle with rotating inertia at each component

The moment of inertia of wheel/tire assembly is given by (6).

$$J_w = m_w r_e^2 + m_t r_t^2 \quad (6)$$

Fig 2 shows the basic idea of rotating inertia which is used to build the dynamic model of the vehicle. The output power is generally less than the input power except that there is no translating acceleration, because it has its own rotating inertia. Due to this rotating inertia, certain amount of power can be stored to the rotating object and the rest of power comes out through the output shaft. On the other hand, the stored power can be discharged in deceleration and it can be captured and stored to a storage system. Note that, in deceleration, the direction of angular acceleration [8] becomes opposite to acceleration, but the direction of rotation will remain same as shown in Fig 3.

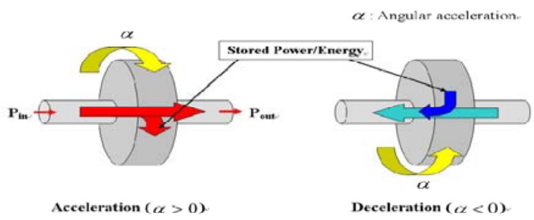

Fig 3 Basic concept of rotating inertia

The tractive force is given by (7).

$$F_T = F_A + F_r + \{ m_e' + \frac{J_M N_T^2 N_F^2}{r_w^2} + \frac{J_c N_T^2 N_F^2}{r_w^2}\} * a \quad (7)$$

The effected of grade force is not included in (7).

6) Power Require To Propel The Vehicle: Fig 4 shows the power flow of a FWD. The total tractive power required to propel the vehicle is given by (8).

$$P_T = V(F_A + F_r + \{ m_e' + \frac{J_M N_T^2 N_F^2}{r_w^2} + \frac{J_c N_T^2 N_F^2}{r_w^2}\} * a) \quad (8)$$

The total tractive power, P_T, is slightly different from the actual tractive power required to propel a vehicle from a power source [8]. Power output from the wheel/tire assembly during propulsion is given by (9).

$$P_{WO} = V\{F_A + F_r + m_v a\} \quad (9)$$

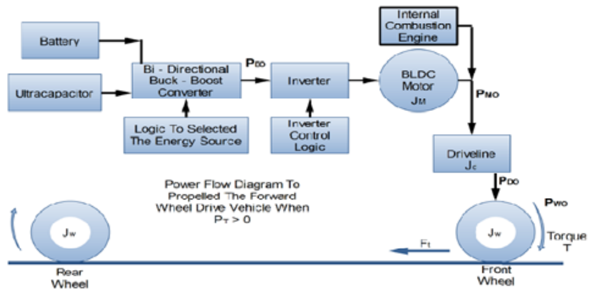

Fig 4 Power flow diagram of FWD vehicle

In order to propel the vehicle and driven wheels, it needs more power to overcome the rotating inertial force of wheel/tire assemblies. Thus the rotating inertial power of wheel/tire assemblies could be added to the actual tractive power. The power output from driveline is given by (10).

$$P_{DO} = V\frac{1}{\eta_f}\{F_A + F_r + (m_v + 4\frac{J_w}{r_w^2})a\} \quad (10)$$

The power output from the motor and ICE which includes the efficiencies of the transmission and the final drive, and the rotating inertial power is given by (11) and (12).

$$P_{MO} = \frac{V}{\eta_t \eta_f}[\{F_A + F_r + m_e' a] \quad (11)$$
$$P_{ICEO} = \frac{V}{\eta_t \eta_f}[\{F_A + F_r + m_e' a] \quad (12)$$

Finally considering efficiency and the rotating inertial power of M/G and ICE yields the actual tractive power required to propel the whole vehicle including rotating components is given by (13) and (14).

$$P_{EO} = \frac{V}{\eta_{M/G}}[\frac{1}{\eta_t \eta_f}[\{F_A + F_r + m_e' a] + \frac{J_M N_T^2 N_F^2}{r_w^2} a] \quad (13)$$
$$P_{ICEI} = \frac{V}{\eta_{ICE}}[\frac{1}{\eta_t \eta_f}[\{F_A + F_r + m_e' a] + \frac{J_c N_T^2 N_F^2}{r_w^2} a] \quad (14)$$

From the P_{EO} the energy output from the energy storage unit E_{EO} can be obtained by integrating P_{EO} over the time period of a drive cycle.

$$E_{EO} = \int_0^T P_{EO}\, dt \quad (15)$$

7) Power Losses During Propulsion: The power losses at driveline, M/G and ICE are given by (16), (17), and (18).

$$\mathbf{P_{DL}=(1-\eta_t\eta_f)\frac{V}{\eta_t\eta_f}[\{F_A+F_r+m_e{'}a]} \quad (16)$$

$$\mathbf{P_{ML}=(1-\eta_{M/G})\frac{V}{\eta_{M/G}}[\frac{1}{\eta_t\eta_f}[\{F_A+F_r+m_e{'}a]+\frac{J_M N_T^2 N_F^2}{r_w^2}a]} \quad (17)$$

$$\mathbf{P_{ICEL}=(1-\eta_{ICE})\frac{V}{\eta_{ICE}}[\frac{1}{\eta_t\eta_f}[\{F_A+F_r+m_e{'}a]+\frac{J_c N_T^2 N_F^2}{r_w^2}a]} \quad (18)$$

8) Regenerative Brake Power and Energy: In order to capture the regenerative brake power/energy, the value of $\mathbf{P_T}$ should always be negative. For example, if the tractive power from the M/G is less than the road load but not zero, then the vehicle being decelerated because there is not enough tractive power to accelerate the vehicle. In this situation, the regenerative brake system cannot capture the regenerative [8, 9,10] brake power/energy.

Thus when the value of $\mathbf{P_T}$ is negative, the power input into the energy storage unit, which is available to be captured from the regenerative braking can be calculated. Multiplying it by a regenerative brake ratio and final drive, transmission and motor efficiencies for each term yields the power input into the storage unit. Fig 5 show the schematic configurations of power flow of regenerative braking for FWD.

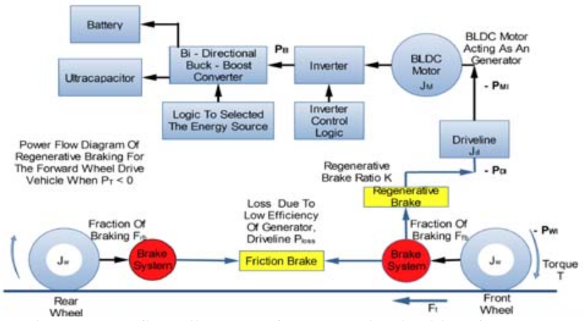

Fig 5 Power flow diagram of regenerative braking for FWD vehicle during braking

The power input into the wheel/tire assemblies at ground, $\mathbf{P_{WI}}$ by braking is given by (19).

$$\mathbf{P_{WI} = V\{\, F_A + F_r + m_v a\}} \quad (19)$$

The brake power required at the driven wheels during braking is given by (20) considering the effect of wheel inertia and brake fraction coefficient f_b.

$$\mathbf{P_{BI} = f_b\, V\, \{\, F_A + F_r + (m_v + 4\,\frac{J_w}{r_w^2})\, a\}} \quad (20)$$

The power input to the drive line is given by (21), where k is the regenerative brake fraction.

$$\mathbf{P_{DI} = kf_b V\{\, F_A + F_r + (m_v + 4\,\frac{J_w}{r_w^2})\, a\}} \quad (21)$$

Applying final drive and transmission efficiencies and adding the rotating inertial power of driveline gives the power input into the generator [4] which can be captured from the driven axles is given by (22).

$$\mathbf{P_{MI}=\eta_t\eta_f V[kf_b V\{F_A+F_r+(m_v+4\frac{J_w}{r_w^2})a\}+\frac{J_d N_T^2 N_F^2}{r_w^2}a\,]} \quad (22)$$

The power input into the storage unit by regenerative braking, $\mathbf{P_{EI}}$ is given by (23).

$$\mathbf{P_{EI}=\eta_{M/G}P_{MI}+\eta_{M/G}V\,\frac{J_M N_T^2 N_F^2}{r_w^2}a} \quad (23)$$

9) Power Losses During Regenerative Braking: The power loss during regeneration including all stages of power loss is given by (24).

$$\mathbf{P_R=(1-\eta_{M/G})[\,P_{MI} + \eta_t\eta_f V\{\frac{J_M N_T^2 N_F^2}{r_w^2}a\}]} \quad (24)$$

The torque of M/G and ICE is given by (25) and (26).

$$\mathbf{T_{M/G} = \frac{P_{MO}}{\omega_{M/G}}} \quad (25)$$

$$\mathbf{T_{ICE} = \frac{P_{ICEO}}{\omega_{M/G}}} \quad (26)$$

IV. Measurement Of Real Time Indian Drive Cycle

The drive cycle is developed for the three different Indian roads which reflect existing traffic conditions. The uniqueness of this methodology is that the drive cycle is constructed considering five important parameters of the time–space profile. These parameters are acceleration, deceleration, idle, cruise, and the average speed [5,6,7]. Measurement of the drive cycle consists of 1) hardware arrangement, and 2) the actual measurement of driving data and construction of drive cycle.

1) Hardware Arrangement: Fig 6 represents the schematic block diagram for measurement of speed of the vehicle under test.

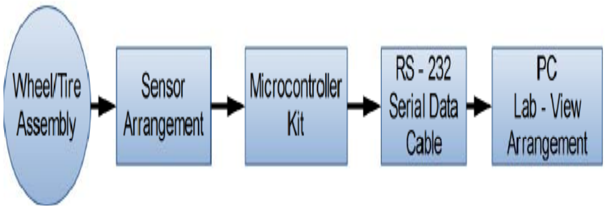

Fig. 6 Block diagram for speed measurement

Real time speed measurement for different types of Indian road is done with the help of speed sensor, data acquisition system with LABVIEW and microcontroller as show in Fig 7 and 8.

Fig. 7 Slotted disc and sensor arrangement for speed measurement.

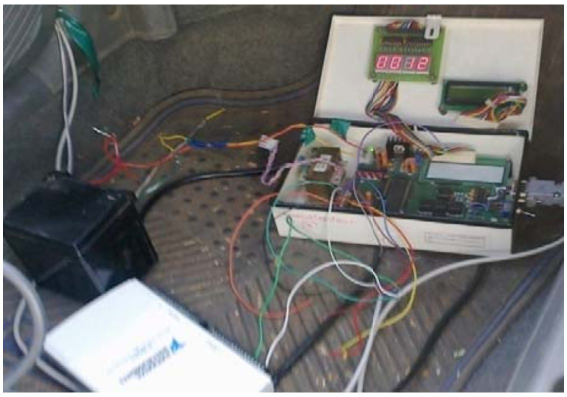

Fig. 8 DAQ card, microcontroller and PC interfacing assembly for speed measurement

Speed sensor is design using a slotted disc of 60 slots and it is mounted on the wheel of the car with an optical hall sensor (MOC 7811) as shown in Fig 7. The hall sensor output is directly feed to DAQ card and microcontroller. The output of DAQ and microcontroller is interface with PC for further analysis as shown in fig 8.

2) Measurement Of Driving Data And Construction Of Drive Cycle: The speed information available from the output of the DAQ card and microcontroller is sent to the PC via RS232 serial cable at every second in the form of revolutions per second (rps).The information is now processed in LABVIEW where the conversion of speed from rps to Km/hr will be done. This procedure is carried out repetitively to obtain large amount of data. The vehicle speed with respect to time should be measured and recorded on all the selected routes during peak and off peak period for varying traffic conditions. Finally the data of velocity profile is plotted with respected to time using the graphical plot inside LABVIEW.

Fig 9 show the Indian city drive cycle (ICDC) for surat city taken during peak hours where large variation in speed is observed. Fig 10 shows the Indian highway drive cycle (IHDC) for Indian national highway 8 (NH-8).Initially the vehicle is accelerated at the very high rate as shown in Fig 10. Fig 11 shows the Indian expressed highway drive cycle (IEHDC) for Baraoda-Anand expressed highway EXP-1. For the maximum period of IEHDC the car is driven between 80 and 90Km/hr.

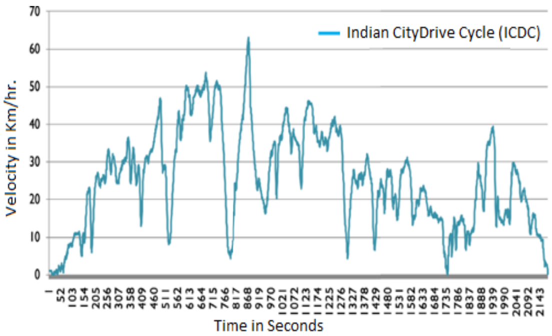

Fig. 9 Indian City Drive Cycle (ICDC)

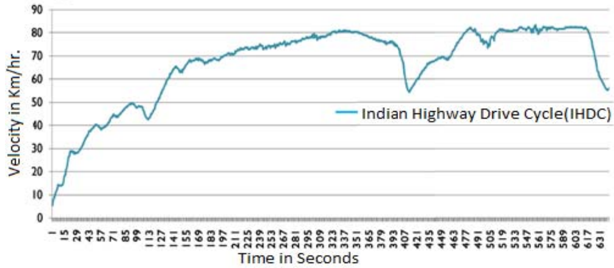

Fig. 10 Indian Highway Drive Cycle (IHDC).

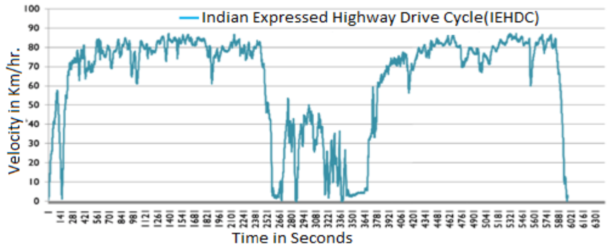

Fig. 11 Indian Expressed Highway Drive Cycle (IEHDC)

V. Vehicle Specification, Operating Modes And Control Mechanism

Parallel HEV configuration is selected for the study as shown in Fig 2 and 4. The vehicle dynamic block is simulated in LABVIEW for three different measured drive cycle on Indian road using vehicle data as shown in table 1.

TABLE I
SPECIFICATION OF VEHICLE

M_V (Kg)	1050	C_d	0.417
A (m^2)	2.1004	C_{rr} , C_{rf}	0.01
m_w (Kg)	5	N_T	variable
r_w (m)	0.265	N_F	4.338
m_t (m)	3		0.95
r_t (m)	0.18		0.95
J_w ($Kg - m^2$)	1.224	f_b	0.6
J_M+J_d ($Kg - m^2$)	1.224	K	0.5

Estimation of components sizing is proposed based on real time Indian drive cycle information, dynamic model of the vehicle and efficient selection of the power sources using power spilt mechanism. The components of the vehicle are sized to meet the desired vehicle performance over different drive cycles with below mentioned operating modes of HEV with effective power distribution between the motor and engine [1,3,13].The selection of the battery and ultracapacitor are dependent on the average power and pulse power demanded by the vehicle. The vehicle operating modes are given below:

1) electric mode only, drawing the power required to propel the vehicle from battery and ultracapacitor,

2) Engine only mode, engine operates close to its best efficiency and surplus power is used to charged the battery/ultracapacitor.

3) Engine plus motor mode, engine operates close to its best efficiency and extra power is supplied by motor.

4) Regenerative braking mode, where the braking energy returns to energy storage devices by operating the motor as a generator.

HEV designers attempt to design a good control mechanism that will increase the fuel economy, reduce ICE emissions and accomplish charge sustainability of the energy pack of the vehicle. For city drive cycle the electric motor supplies the acceleration power through ultracapacitor (transient power) and average power through battery. Under regenerative braking mode electric motor acts as a generator and supplies power back to ultracapacitor and battery. For highway and express highway drive cycle the electric motor supplies initial acceleration (transient power) through ultracapacitor and steady state power is supplied by the ICE. The ICE may charge the battery/ultracapacitor, depending on the availability of extra power and battery/ultracapacitor state of charge. The main goal of these control techniques is to size HEV components so that the ICE operates efficiently and the battery life gets extended by the use of an ultracapacitor under different Indian road conditions.

The size of the battery pack is dependent on two factors. First, the battery pack should be capable of delivering motor average power [2]. Second, in case of charge sustainable HEVs, the battery energy should meet the requirement of keeping battery state of charge within a specified limit. (For charge depleting EV/HEV, the size of battery pack depends on the vehicle range specification). In this paper, for a selected drive cycle the power supplied by the battery pack (steady state power) and Ultracapacitor (transient power)at a time t is given by (13).During braking the motor acts as a generator and delivers power back to the energy storage unit at a very fast rate. Due to chemical sluggishness of battery, initially the regenerative energy will be captured by the ultracapacitor as it can be charged at faster a rate. The amount of regenerative power returned back to the supply system is given by (23).The size of motor should be equal to power needed to support the vehicle driving under accelerating mode. Whereas the engine size is based on the power need to drive the vehicle at a constant speed as well as the maximum speed (highway or a expressed highway driving).

VI. Simulation Result

Simulation results for Indian City Drive Cycle (ICDC)

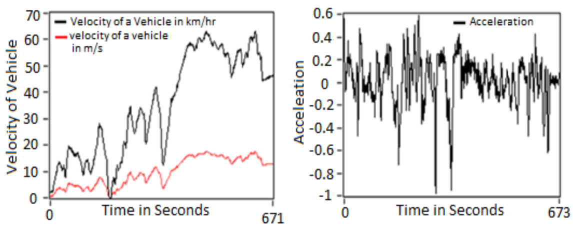

Fig. 12 Velocity and acceleration profile for ICDC.

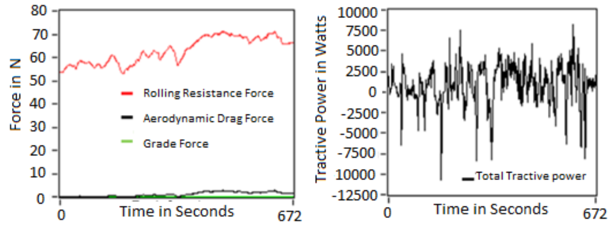

Fig. 13 Force and total tractive power for ICDC

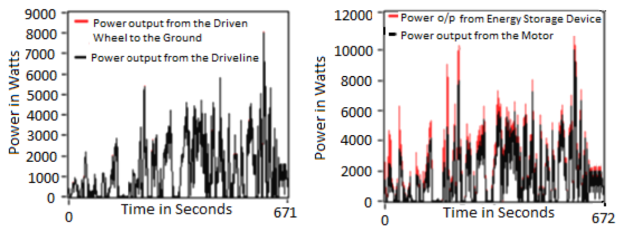

Fig. 14 Power output for propulsion for ICDC

Fig 12 shows the velocity profile for the Surat city drive cycle and its corresponding acceleration/deceleration profile. As the initial rate of acceleration is low in ICDC, the power demanded by the vehicle is also low. The maximum acceleration is only 0.6m/s^2. At a low speed the rolling resistance and the aerodynamic drag force is also small based on which the total tractive power required is low as shown in Fig 13. The power output from different components of HEV is shown in Fig 14.

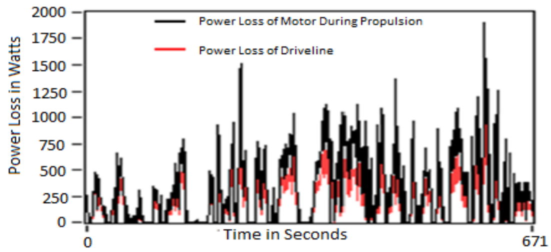

Fig. 15 Power loss in motor and driveline for ICDC

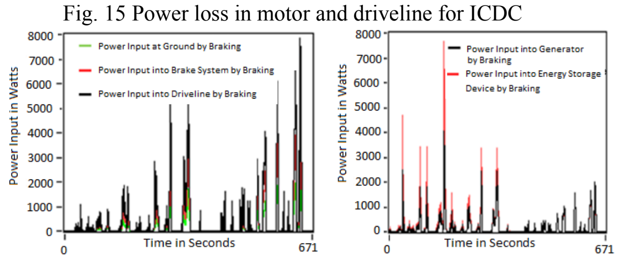

Fig. 16 Power input during regenerative braking for ICDC.

Fig 15 shows the power loss taking place inside motor and driveline for ICDC. Fig 16 shows the power input to the different components of HEV during regenerative braking. For a city drive cycle, large numbers of negative power spikes are generated due to frequent deceleration. This large negative power spike is used to charge the energy storage devices.Simulation result for Indian Highway Drive Cycle (IHDC)

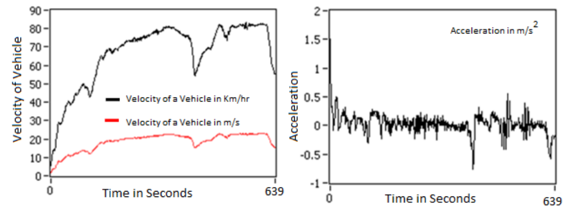

Fig. 17 Velocity and acceleration profile for IHDC

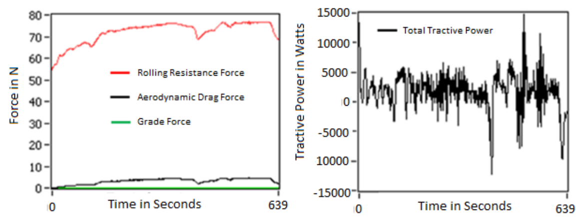

Fig. 18 Forces and total tractive power for IHDC

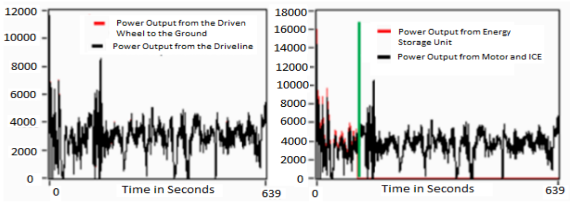

Fig. 19 Power output for propulsion for IHDC

Fig 17 shows the velocity and the acceleration/deceleration profile for IHDC. The vehicle is accelerated at a very high rate (i.e 1.5 m/s^2) and demands a high tractive power of 14 Kw as shown in Fig 18. The power drawn from the energy storage devices is 16 Kw as shown in Fig 19 including the power loss in motor and driveline. Fig 19 shows the power delivered by the motor and ICE and the green line separates the two. This high power demand for a short duration has to be supplied by ultracapacitor. Thus the sizing of ultracapacitor is based on the acceleration power demanded by the vehicle.

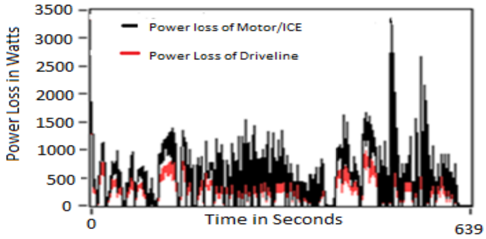

Fig 20 Power loss in motor and driveline for IHDC

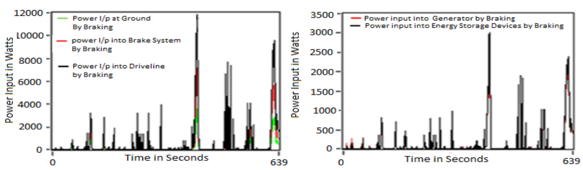

Fig 21 Power input during regenerative braking for IHDC.

Fig 20 show the power loss taking place inside motor and the driveline during propulsion. Due to high initial rate of acceleration the motor demands a high current. As a result of the high current large i^2r losses occur in the motor. The power loss inside the driveline is due to the inertia of different rotating components. This loss is stored in the form of kinetic energy in the rotating unit. This stored energy is feedback at the time of braking. Fig 21 shows the power input to the different components of HEV during regenerative braking. The maximum regenerative power peak of 10.4 kwatts is generated as shown in Fig 21.

Simulation result for Indian Express Highway Drive Cycle (IEHDC)

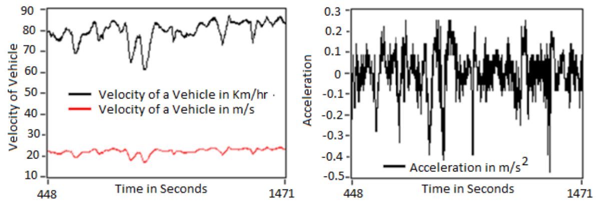

Fig. 22 Velocity and acceleration profile for IEHDC.

The Indian express highway drive cycle (IEHDC) is measured on the expressed route between Baroda and Anand district. This drive cycle is simulated for 448 to 1471 seconds where the speeds range is of 80 to 90 km/hr range.

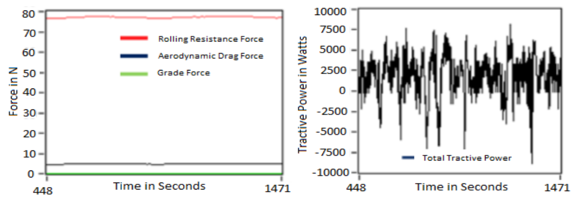

Fig. 23 Forces and Total Tractive Power For IEHDC.

Fig 22 shows the velocity and acceleration/deceleration profile for time duration of 448 to 1471 seconds. During this period the change in the speed of the vehicle is small and there is no rapid acceleration taking place. Fig 23 shows the different forces acting on the vehicle and the total tractive power needed to maintain the constant velocity. As the variation in velocity is small, the variation in the rolling resistance force is small and has a value in the range of 75 to 80 N.

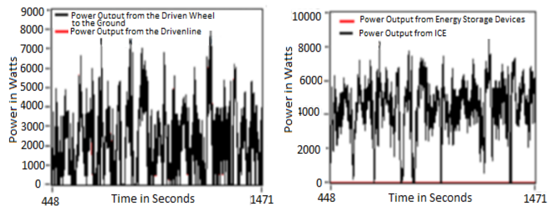

Fig. 24 Power Output For Propulsion For IEHDC.

Fig 24 shows the power output from various components of HEV for IEHDC. It shows that the average power required is 5000 watts.

International Journal of Information, Control and Computer Sciences
ISSN: 2517-9942
Vol:5, No:10, 2011

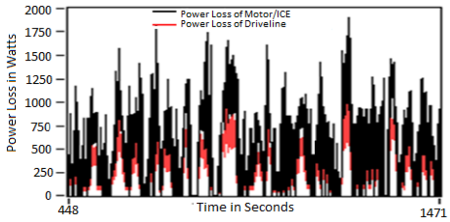

Fig. 25 Power Loss In Motor And Driveline For IEHDC.

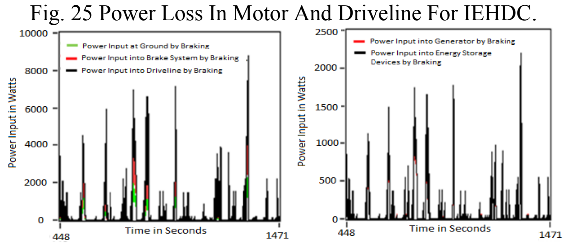

Fig. 26 Power Input During Regenerative Braking For IEHDC.

Fig 25 shows the power loss inside motor and driveline. Fig 26 shows the power input to the different components of HEV during regenerative braking. As the vehicle is driven on the express road, the negative power spike is of a lower value compared to the ICDC.

VII. Selection And Estimation Of The Rating Of HEV Componants

Vehicle performance under three different indian real time drive cycles is shown in Table II and III. From the simulation results the power requirement is dependent on the velocity and rate of acceleration of the vehicle.The estimation of the vehicle components is based on a generlized approach considering the maximum power demand of the vehicle for the three measured drive cylces, so that the vehicle operates at the best possible efficiency under diverse driving conditions.

In this study the initial acceleration is provided by the electric motor through energy storage device. The power required by the vehicle operating under the three indian drive cycle during starting are 5420watt, 15000watts, 11000watts respectivly. As this power is required for a short duration, the battery size and wieght increase which decreases the efficiency of battery operated HEV/EV.Choice of a pulse power device like ultracapacitor's can resolve this problem as the wieght and size of an ultracapcitor is lower than the battery for the same power demand.The size of ultracapcitor is based on the maximum acceleration power demanded by the vehicle for any of the three drive cycles.

For an ICDC, the battery sizing is based on the average power demanded by the vehicle plus auxillary power. Thus the total power requirement is nearer to 4000watts.

For an IHDC and IEHDC, the size of engine is based on summation of the average power demanded by the vehicle, the power requried to maintain the battery SOC at a safe level and auxillary power. Thus the total power requirement is nearer to 15Kw considering the engine efficiency of approximately 40%.For higher acceleration during driving if the power demanded by the vehicle is more than the engine capacity then the extra power is supplied by the electric motor.

Since the acceleration during starting is provided by the electric motor, the peak power rating of electric motor is based on the maximum peak power demanded by the vehicle. Based on the rating of the electric motor and ultracapaitor, power rating of the inverter and converter are estimated cosidering the switching and conduction losses of the power electronics devices.

During regeneration, the kinetic energy stored in the rotating components of the vehicle is converted into electrical energy by operating the motor as a generator. This generated electrical energy is stored in the energy storage device. It is observed from the simulation result that during ICDC the regenerated power is more than in the case of IHDC which in turn is higher than IEHDC. This is due to the fact that the frequency and rate of deceleration is highest in ICDC.

Based on the above, the estimation of component sizing for the vehicle to be hybridized is carried out and is presented in table IV and V.

TABLE II
Results Of Simulation For Three Drive Cycle

Drive cycle	Duration of drive cycle	velocity in Km/hr	Peak power during drive cycle (Watts)	Average power during drive cycle
ICDC	2161	65	10500	2000
IHDC	631	85	11000	2500
IEHDC	6274	93	12000	4000

TABLE III
Result Of Simulation For Three Drive Cycle

Drive Cycle	Initial accelera-tion in m/s^2	Initial power output from energy storage unit (Starting from zero speed)	Initial Starting Torque (N-m)	Peak regenera-tive power during drive cycle (watts)
ICDC	0.55	4520	40	7700
IHDC	1.5	15000	98	3000
IEHDC	1.3	11000	80	2200

TABLE IV
Rating Of Energy Storage Device For HEV

Energy Storage System	Battery	Ultracapacitor
ModuleCapacity/ Maximum Voltage	80Ah/12V	167 F/48V
Module Mass (Kg)	12 - 15 Kg	8 Kg
Quantity Configuration	4 in Series	2 Parallel
System Nominal Voltage	48 Volts	48 Volts

TABLE V
MOTOR AND POWER ELECTRONIC DETAIL FOR HEV

Motor	15Kw peak power, 48Volts, 1500rpm, 100 N-m
ICE	15 Kw, 2500 rpm
Power Electronics Interface	---
Peak Power	18 Kwatts
Dc Buss Voltage	48-50 Volts
Switching Frequency	20 KHz
Thermal Dissipation Mode	Air Cooled Heat Sink

VI CONCLUSION

India is a country with dense population and diverse types of roads and road conditions. Under such road conditions the vehicle operates with high emissions and fuel consumption. Hence in this paper an attempt is made to design and estimate the size of HEV components for different driving patterns of Indian roads (urban, highway and expressway) , so as to reduce the emissions and fuel consumption of the vehicle, with the same performance as that of a conventional vehicle.

The vehicle component ratings are estimated based on virtual testing of the vehicle in LABVIEW using power split mechanism and proper selection of operating modes of the vehicle. In this analysis, increase in the overall mass of the test vehicle due to rotating inertia and the actual variation of acceleration, deceleration and speed of the vehicle has been considered to estimate the performance and sizing of vehicle components. Due to above consideration the calculated power demand of the vehicle under test is more accurate and near to the power demand of the actual vehicle operated on the road.

Even under regeneration, the stored kinetic energy of each rotating component starting from wheel to electric motor will be used to charge the energy storage device. This helps to size the vehicle components more realistically.

The reduction of emission is achieved by supplying the initial acceleration power by the electric motor. A combination of ultracapacitor with a battery helps to reduce the size of battery as well as the overall weight of the vehicle.

ACKNOWLEDGEMENT

We are thankful to Department of Electrical Engineering, SVNIT Surat for their kind academic support.

REFERENCES

[1] Jonas Hellgren, and Erik Jonasson, " Maximisation of brake energy regeneration in a hybrid electric parallel car" Int. J. Electric and Hybrid Vehicles, Vol. 1, No. 1, 2007.

[2] Michael Panagiotidis, George Delagrammatikas, and Dennis Assanis, "Development and use of a regenerative braking model for a parallel hybrid electric vehicle," SAE 2000-01-0995.

[3] G. Steinmauer and L. d. Re, "Optimal control of dual power sources" presented at Proceedings of the IEEE International Conference on Control Applications, CCA '01,2001.

[4] YiminGao, Liping Chen, and Mehrdad Ehsani, "Investigation of the effectiveness of regenerative braking for EV and HEV," SAE 1999-01-2910.

[5] Stefano d'Ambrosio, EzioSpessa, "Methods for Specific Emission Evaluation in Spark Ignition Engines Based on Calculation Procedures of Air-Fuel Ratio: Development, Assessment, and Critical Comparison" Journal of Engineering for Gas Turbines and Power, Vol. 127, OCTOBER 2005.

[6] E.tzirakis, K.pitsas, F.zannikos and S.stournas, "Vehicle Emissions and Driving Cycles: Comparison of the Athens Driving Cycle (ADC) with ECE-15 and European Driving Cycle (EDC)" Global NEST Journal, Vol 8, No 3, pp 282-290, 2006.

[7] Sanghpriya H. Kamble, Tom V. Mathew, G.K. Sharma, "Development of real-world driving cycle: Case study of Pune, India" International Journal of Vehicle Design 18, 391–399.

[8] Dr.N. K. Giri, " AutomobileTechnonlogy", Khanna Publishers, New Delhi, First Edition 2008.

[9] Gino Sovran, and Dwight Blaser, "A contribution to understanding automotive fuel economy and its limits," SAE 2003-01-2070.

[10] YiminGao, and MehrdadEhsani, "Electronic braking system of EV and HEV – integration of regenerative braking, automatic braking force control and ABS," SAE 2001-01-2478.

[11] J. M. Miller, Propulsion Systems for Hybrid Vehicles: IEE, ISBN 0-86341-336-6, 2004.

[12] Milkins, E. and H. Watson., "Comparison of Urban Driving Patterns, Motor vehicletechnology: Progress and Harmony", The Second International Pacific Conference onAutomotive Engineering, Tokyo, Japan, SAE of Japan, Inc. (1983), p. 735-746.

[13] Z.Rahman, K.L.Butler and M.Ehsani., "A Study Of Design Issues On Electrically Peaking Hybrid Electric Vehicle For Diverse Urban Driving Patterns."Society of automotive engineers, 1999-01-1151.